Anisotropic 2D and 3D averaging of fMRI signals

Andres Fco. Solé, Shing-Chung Ngan, Guillermo Sapiro, Xiaoping Hu, and Antonio López

Abstract— **A novel method for denoising functional MRI temporal signals is presented in this note. The method is based on progressively enhancing the temporal signal by means of adaptive anisotropic spatial averaging. This average is based on a new metric here proposed for comparing temporal signals corresponding to active fMRI regions. Examples are presented both for simulated and real two and three dimensional data. The software implementing the proposed technique is publicly available for the research community.**

Keywords— **Functional MRI, anisotropic averaging, Fourier spectrum, signal metrics.**

I. Introduction

Functional Magnetic Resonance Imaging (fMRI) is the most significant and revolutionary advance in MRI in recent years, e.g., [1], [2], [3]. This technique uses MRI to non-invasively map areas of increased neuronal activity in the human brain without the use of an exogenous contrast agent. The majority of fMRI experiments are based on the blood oxygenation level dependent (BOLD) contrast, which is derived from the fact that deoxyhemoglobin is paramagnetic, and changes in the local concentration of deoxyhemoglobin within the brain lead to alterations in the magnetic resonance signal. It is generally assumed that neuronal activation induces an increase in regional blood flow without a commensurate increase in the regional oxygen consumption rate (CMRO2) in which case the capillary and venous deoxyhemoglobin concentrations should decrease, leading to an increase in T2* and T2. This increase is reflected as an elevation of intensity in T2*- and T2-weighted MR images.

Functional MRI has better spatial resolution than other non-invasive techniques like EEG (electroencephalography) or MEG (magneto encephalography). On the other hand, it has poorer time resolutions. This restriction on time resolution and the low signal to noise ratio (SNR) of fMRI images makes necessary the use of well designed data acquisition protocols. Two classes of protocols are popular, the periodic or block-design and the event-related one. In the periodic paradigm the subject alternates between periods of stimulation and rest, which usually have the same time duration. In this case each pixel/voxel of the fMRI data consists of a time series which can be divided in epochs, an epoch being the period of time (images) which corresponds to activity or rest. Thus the data can be considered "periodic" where the "period" is just the epoch duration. In the case of event-related paradigms the subject realizes the activity only during a short period of time, i.e., a trial, and the trial can be repeated in a periodic or random fashion. The work described here is tuned to block design protocol on periodically repeated event related protocols, though many of the concepts here introduced can be extended to event-related experiments as well.

Much work on analyzing, denoising, and clustering active regions in fMRI volumes has been reported in the literature. The problem consists on cleaning the data and determining which voxels belong to activated zones of the brain, see for example [4], [5], [6], [7], [8], [9], [10], [11], [12], [13]. In this note we present a novel technique based on anisotropic (selective) spatial averaging of time series. The data enhancement and estimation of active voxels is progressively improved. The improvement is based on comparing, using a metric introduced in this paper, the time series of unclassified voxels with those of previously classified ones. This technique will be detailed in the rest of this paper. The software is publicly available for the research community at http://www.ece.umn.edu/users/guille.

Andres Fco. Solé: Centre de Visió per Computador, Universitat Autonoma de Barcelona, Edifici O, Spain

Shing-Chung Ngan: Center for Magnetic Resonance Imaging, University of Minnesota

Guillermo Sapiro (corresponding author): Electrical and Computer Engineering, University of Minnesota, Minneapolis, MN 55455 (guille@ece.umn.edu)

Xiaoping Hu: Center for Magnetic Resonance Imaging, University of Minnesota

Antonio López: Centre de Visió per Computador, Universitat Autonoma de Barcelona, Edifici O, Spain

II. Selective averaging of time-series

Different methods have been reported in the literature for noise removal in fMRI, e.g., [14], [15], [16], [17]. We now discuss our approach.

A. Isotropic averaging

If multiple copies of the signal, all corrupted with the same type of noise, are available, the simplest way to denoise the signal is to average among its repetitions.[1] There are different standard ways to do this average. For instance, let us consider a standard $N \times N$ grid where each cell (i, j) contains one instantiation of the time signal $x_{i,j}(t)$. One way to obtain an averaged version $\tilde{x}_{i,j}(t)$ of the signal at the cell (i, j) is to replace it with the signal obtained by averaging the original signal with all its neighbors by

$$\tilde{x}_{i,j}(t) = \frac{1}{9} \sum_{a=i-1}^{i+1} \sum_{b=j-1}^{j+1} (x_{a,b}(t)), \tag{1}$$

where we have used a simple 3×3 neighborhood. The obvious problem with this kind of *filtering* is that if we have signals of different classes (e.g., active and non-active voxels), the averaging process will merge them, leading to an undesired result. The problem of merging signals of different classes is well known and sometimes it is called *blurring* in the literature. We can improve the averaging process simply by multiplying each neighbor by a positive factor (weight≥ 0) before averaging. Different selections on the weights will lead to different *smoothing* results. Usually the weights are selected to be constant and one way to represent it is by a matrix or *mask* (in our case a 3×3 matrix) where each cell represents one weight. We obtain in this way a *weighted* average, the entries of the mask are just the weights assigned to each of the neighbors of the cell (i, j). When the weights are selected to be constant, the average processing is an *isotropic average* or *stationary average*, all the cells in the grid are treated in the same way. This kind of average processing works when all the time series on the neighborhood are of the same class or when there is not much concern about the mixing of different kind of signals. This is of course not the case of fMRI, where we can have active and non-active pixels/voxels in the same neighborhood.

B. Anisotropic averaging

When we want to make a selective averaging of the signals we have to use specific weights for each cell of the grid. That means that the weights are based on some kind of measure (metric) concerning the specific neighbor and the cell being averaged. In our case we will call this measure a *confidence* measure, and

$$\tilde{x}_{i,j}(t) = \sum_{a=i-1}^{i+1} \sum_{b=j-1}^{j+1} (w_{a,b} x_{a,b}(t)). \tag{2}$$

In (2) the term $w_{a,b}$ is determined by a confidence measure involving the signal being averaged $x_{i,j}$ and its corresponding neighbor $x_{a,b}(t)$. Note then that the weights are position dependent, and the averaging is *anisotropic* or *non-stationary*. We can represent the confidence measure as a scalar function which takes as inputs two time signals and returns their similarity:

$$w_{a,b} = \psi(x_{i,j}(t), x_{a,b}(t)). \tag{3}$$

It is this confidence measure which will allow us to distinguish between different kind of signals and be able to perform a selective averaging, that is averaging only the signals of the same class. The key problem then becomes the design of the confidence measure. In our case of fMRI signal processing, we have two different signals to treat, concretely the activity signal and the rest one.[2] These signals are very noise and the percentage of change between an activate signal and a non activated one is at most 10%. We have then to distinguish two quite similar signals, both of them very noisy, and to assign a measure of similarity. It seems adequate then to use a probabilistic measure between the signals and to use this probability measure as a confidence measure for our weighted average. We proceed to describe this now.

C. The confidence measure

Different work, e.g., [14], [6] had suggested that the activation information of the fMRI signal is concentrated in the low frequencies. In fact, Mitra et al. [14] had demonstrated how the low frequencies contain the information of both the activation pattern and physiological noise. We considered the use of the (time) Fourier spectrum of the data in order to construct the similarity measure between the time signals. This has two main advantages: First, the Fourier spectrum is invariant under translation of the signals, which makes our measure invariant to possible time displacements of the activation pattern. Second, we can consider only the low frequency information rejecting the high frequencies which are mainly due to noise. Due to the periodicity of the stimuli in the paradigm, we can expect the signal corresponding to

[1] Under simple conditions, averaging is actually the optimal estimator of the original signal.

[2] In this note we consider only one class including all active pixels, though the activation pattern in the class can vary, see below. The extension of the work here presented, to allow for more than one class, is the subject of current research.

activity to be pseudo-periodic also. In fact our signal is composed of periods of rest and activity or *epochs* of approximately equal length (there is a repetition, though the signal repeating does not have to be exactly the same). If we look at the spectrum of such a signal formed of **n** epochs we can observe that the highest contribution in frequency corresponds to the n-frequency of the Fourier decomposition, and to its multiples. In the left side of Fig. 1 we can observe the simulation of this type of behavior.

One way to construct a similarity measure between our signals is to consider them as points in certain space and then define a metric in this space, giving the notion of distance between signals. The first step is to define an adequate space. Consider a signal $x(t)$ composed of k epochs and denote by $X(w)$ its Fourier spectrum. We can remove the first value of the Fourier spectrum which corresponds to the average value of $x(t)$ and does not carry any frequency information. Since we are interested only in the low frequency information we can also simply cut off the Fourier spectrum by discarding the high frequency information which is mainly noise as pointed out in [14]. We simply take the first $5k$ elements of the Fourier spectrum, which assures that all the low frequencies are taken into account. We denote as $\tilde{X}(w)$ this truncated Fourier spectrum of the signal. Since $\tilde{X}(w)$ contains the low frequency information of the signal it seems appropriate to define our space as the one generated by this truncated Fourier spectrums, which is a $5k$-dimensional space. We are actually not interested in the whole space, as we are just interested in the subspace corresponding to the spectrums of the activated voxels. One way to obtain this subspace is by constructing its covariance matrix from a sample of activated voxels. Our approach consists of detecting some (clearly) activated voxels, simply by using a correlation with a box-car function, and then use these voxels to construct the covariance matrix. We can fix the threshold value of the correlation in order to detect only highly activated voxels making sure that non activated voxels are not included in our initial set. First of all we normalize our initial set using the Euclidean norm in $\Re^{5k}$ and then subtract the average vector of the normalized set to each normalized vector. Denote by H the matrix whose columns are formed by the normalized 0 mean cut spectrums of the initial set of activated voxels (we will denote this initial set as Ω). Then the covariance matrix of the data is simply HH^T. This $5k \times 5k$ symmetric matrix is then diagonalized in order to obtain an orthonormal representation of our space, say $HH^T = P^T D P$, where P is formed by the eigenvectors of the decomposition and D is a diagonal matrix whose elements are the corresponding eigenvalues. We can think about the eigenvalues as a measure of the information that each eigenvector contribute in the description of the subspace formed by the initial set of points. The goal is to select only those eigenvectors whose eigenvalues are significant. The usual way to do this is by selecting the minimum number of eigenvalues necessary to obtain a certain percentage of the total information contained by the whole set of eigenvalues, usually a 90% is used. Once the eigenvalues are ordered in a descending order we can obtain the most relevant eigenvalues by selecting the minimum l which obeys

$$\frac{\sum_{i=1}^{l} \lambda_i}{\sum_{\text{all eigenvalues}} \lambda_j} \geq 0.9. \tag{4}$$

The eigenvectors associated with the selected eigenvalues are then a good low dimensional representation of the subspace we are interested in. Defining $\tilde{P}$ and $\tilde{D}$ as the matrices of the selected eigenvectors (in columns) and eigenvalues respectively, we can define the Mahalanobis distance in our subspace by

$$d_S(x,y) = (\tilde{X}(w) - \tilde{Y}(w))\tilde{P}D^{-1}\tilde{P}^T(\tilde{X}(w) - \tilde{Y}(w)). \tag{5}$$

The distance of a point $x(t)$ (or the reconstruction error) to the subspace of interest S can be calculated as

$$d(x,S) = \|\tilde{X}\|_2 - \|\tilde{P}^T\tilde{X}\|_2. \tag{6}$$

Finally, we can define the similarity between two voxels $x(t)$ and $y(t)$ as:

$$\psi(x,y) = e^{-[(W_P d(x,S))^2 + (W_P d(y,S))^2 + (W_I d_S(x,y))^2]}, \tag{7}$$

where W_P and W_I are defined as

$$W_P = \frac{\alpha}{\max\limits_{\forall x \in \Omega}\{d(x,S)\}}, \tag{8}$$

$$W_I = \frac{\alpha}{\max\limits_{\forall x,y \in \Omega}\{d_S(x,y) | x \neq y\}}, \tag{9}$$

and α is a parameter which controls the diffusivity of the averaging process.

D. Proposed algorithm

The algorithm is an iterative process which uses the metric (measure) calculation as a feedback process to progressively improve the results. Before beginning to iterate we have to find an initial threshold value

for the correlation coefficient making sure that the initial set of activated voxels do not contain any false positive. The iterative process can be resumed in the following steps:

1. Compute the initial set Ω of activated voxels by thresholding the correlation coefficient.
2. Using the current set of activated voxels, find the metric, W_P and W_I.
3. For each voxel of the grid calculate their averaged voxel using Eq. (2).
4. Update the initial grid substituting each voxel by its averaged version and go to step 1.

This algorithm can be easily extended to 3D data sets simply by modifying the 2D neighborhood of each voxel by its 3D neighborhood.

III. Results

We have evaluated our method both on simulated and real fMRI data. First of all we present an experiment on simulated activation data which was corrupted with real baseline noise. We then test our method on two sets obtained from a 1.5 T scanner. The first data set serves as an example for the 2D smoothing algorithm while the second one was smoothed using the full 3D Euclidean connectivity. Activation maps were obtained before and after the smoothing process showing the performance of the proposed algorithm. The activation maps were constructed by thresholding the correlation coefficient between a box car shaped activation model and each voxel of the image.

The first example shows the performance of the algorithm on a 10×10 grid of simulated data which was obtained by corrupting with real 1.5 T baseline data a fictitious set of activations. In the right hand of Fig. 1 we show the initial spatial configuration and activation pattern used to simulate the activation on the baseline. In Fig. 2 we present the detected activations before and after the regularization process. Note that the holes in the filtered activations are preserved, that is even if a non activated pixel is surrounded by activated pixels it remains non active after the regularization. Finally in Fig. 3 and Fig. 4 we plot the time series corresponding to the activation pattern detected and its immediate neighbors. Note that none of the non activated pixels has been affected by the activated ones during the regularization process.

Now we describe the experiments performed on the real data. The first data set corresponds to an oblique slice ($FA = 55^0$, $FOV = 22 \times 22cm^2$, slice thickness $5mm$) through both the motor and the visual areas of

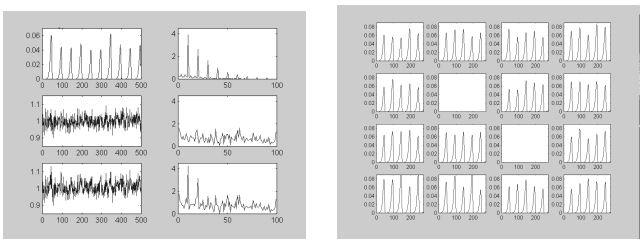

Fig. 1. *Left: from top to bottom simulated data using an exponential function as stimuli (note that each stimuli is different from the previous one), real baseline from a healthy male (no stimulation), simulated data generated by adding the simulated stimuli and the baseline and their corresponding Fourier spectrum (right). Right: Activation pattern used in the grid simulations.*

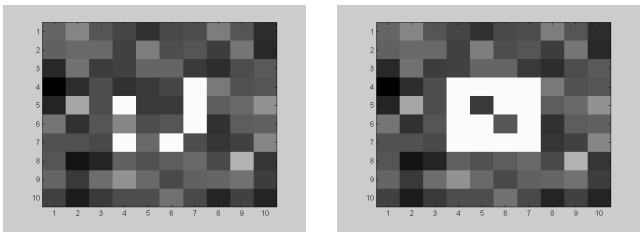

Fig. 2. *Activation map obtained on the simulated grid before (left) and after (right) the 2D smoothing process (initial threshold=0.45, $\alpha = 0.5$, 10 iterations).*

a healthy male. T_2^* weighted echo planar images (EPI) were acquired ($TE = 60ms$, $TR = 300ms$). During the acquisition of the EPI images, the subject was asked to perform right-handed rapid finger movement when flashing LED goggles were on. In each epoch, which lasted 19.2s, the LED goggles were turned on for $5.4s$. The epoch length is equal to 64 images and a total of 31 epochs were acquired.

The second data set consists of three consecutive slices ($FOV = 22 \times 22cm^2$, slice thickness $6mm$)

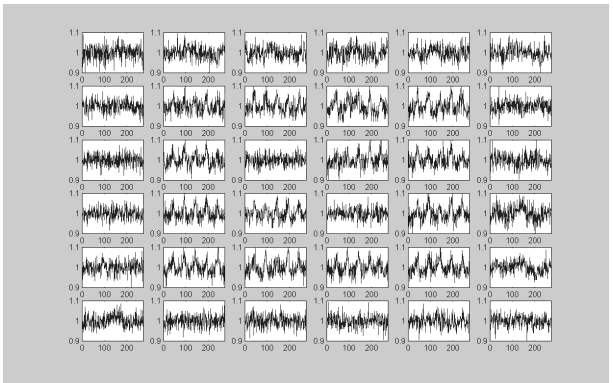

Fig. 3. *Time series corresponding to a 6×6 ROI centered on the grid before regularization.*

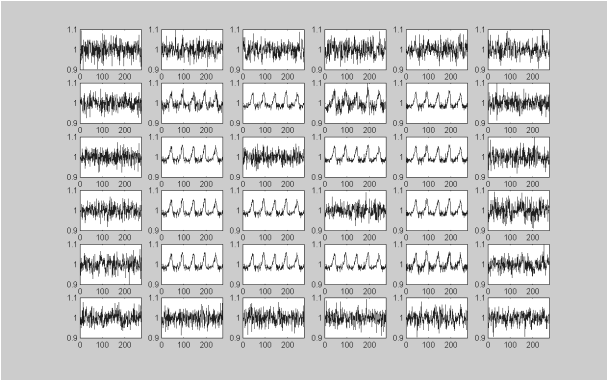

Fig. 4. *Time series corresponding to a 6×6 ROI centered on the grid after regularization.*

from the visual-motor cortex of a healthy female. T_2^* weighted EPI images were acquired ($TE = 60ms$, $TR = 800ms$). During the acquisition, the subject was asked to perform a finger opposition task during a visual stimulation (on time/on time+off time=10/40). The epoch length is equal to 40 images and a total of 19 epochs were acquired.

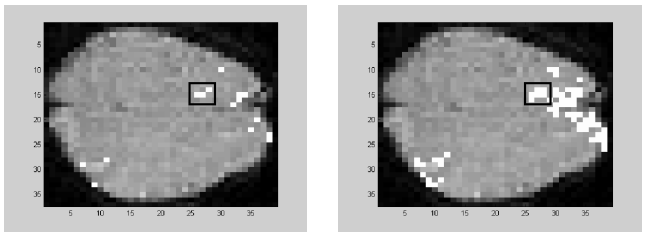

Fig. 5. *Activation map obtained on the male brain before (left) and after (right) the 2D smoothing process (initial threshold=0.5, $\alpha = 0.5$, 10 iterations).*

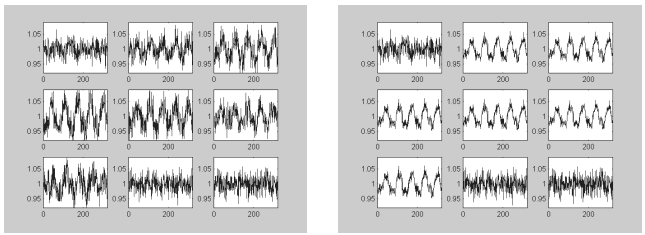

Fig. 6. *Selected ROI of the activation map obtained on the male brain before (left) and after (right) the smoothing process.*

In Fig. 5 we show the activation maps obtained before (left) and after (right) the smoothing process on the male subject. The regularization process leads to a better detection of the activation clusters due to the improvement of the signal to noise ratio. In Fig. 6 we have selected a ROI (see Fig. 5 right) containing one of the clusters which is detected after the smoothing process, and then we have plotted each of the temporal series before (left) and after (right) the smoothing process. One can notice how the signal is enhanced in the smoothed ROI, leading to a better clustering.

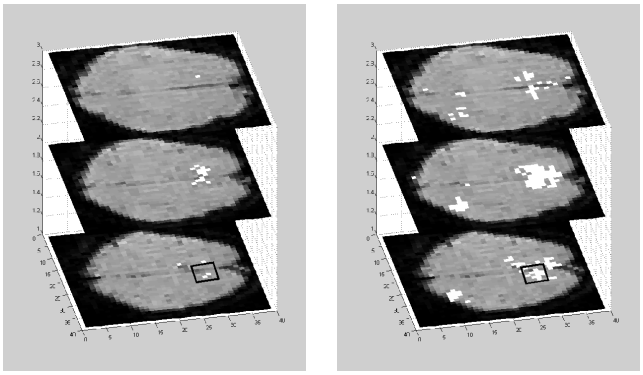

Fig. 7. *Activation map obtained on the female brain before (left) and after (right) the 3D smoothing process (initial threshold=0.5, $\alpha = 0.5$, 10 iterations).*

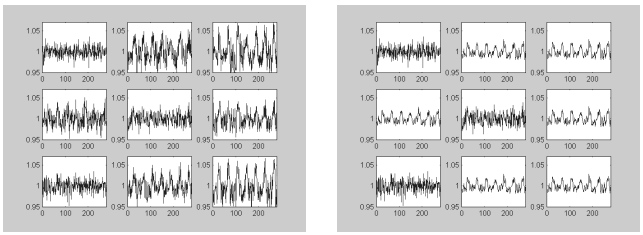

Fig. 8. *Selected ROI of the activation map obtained on the female brain before (left) and after (right) the smoothing process.*

In Fig. 7 we show the activation maps obtained before (left) and after (right) the 3D smoothing process on the female subject. As in the previous case the regularization process leads to a better detection of the activation clusters. In Fig. 8 we have selected a ROI (see Fig. 7 right) containing one of the clusters which is detected after the smoothing process, and then we have plot each of the temporal series before (left) and after (right) the smoothing process. Once again, the signal is enhanced, leading to a better clustering.

IV. Conclusions

A novel method for denoising functional MRI temporal signals was presented in this paper. The method is based on progressively enhancing the temporal signal by means of an adaptive anisotropic spatial averaging. This average is based on a new metric defined for time series corresponding to active fMRI regions. Examples were presented both for simulated and real two and three dimensional data.

We are currently investigating the use of structural MRI to help in the averaging process. The basic idea is to use connectivity information computed with structural MRI, [18], to further specify the averaging neighborhood. We are also currently investigating the metric and concepts here introduced for the enhancement of signals obtained in event-related fMRI. One of the directions is to use the concept of progressive enhancement, which permits to start with a very small set of confident pixels/voxels. Results on these directions will be reported elsewhere.

Acknowledgments

This work was performed while the first author was visiting the ECE Department at the University of Minnesota. We thank Marcelo Bertalmio and David Heeger for interesting conversations. This work was partially supported by a grant from the Office of Naval Research ONR-N00014-97-1-0509, the Office of Naval Research Young Investigator Award, the Presidential Early Career Awards for Scientists and Engineers (PECASE), a National Science Foundation CAREER Award, the National Science Foundation Learning and Intelligent Systems Program (LIS), the National institutes of Health (R21MH59245, P41RR08079, ROIMH55346), and the Generalitat de Catalunya (BE2000).

References

[1] S Ogawa, RS Menon, D Tank, SG Kim, H Merkle, JM Ellermann, and K Ugurbil, "Intrinsic signal changes accompanying sensory stimulation: Functional brain mapping with magnetic resonance imaging.," *Proc. Natl. Acad. Sci. USA*, vol. 89, pp. 5951–5955, 1992.

[2] M Moseley and GH Glover, "Functional mr imaging: capabilities and limitations," *Functional Neuroimaging North American Imaging Clinics*, vol. 5, no. 2, pp. 161–191, 1995.

[3] RBH Tootell, JD Mendola, NK Hadjikhani, PJ Ledden, and AK Liu, "Functional analysis of v3a and related areas in human visual cortex," *Neuroscience Journal*, vol. 17, no. 18, pp. 7060–78, 1997.

[4] C Goutte, P Toft, E Rostrup, FA Nielsen, and LK Hansen, "On clustering fmri time series," *NeuroImage*, vol. 9, no. 3, pp. 298–310, 1999.

[5] BA Ardekani and I Kanno, "Statistical methods for detecting activated regions in functional mri of the brain," *Magnetic Resonance in Imaging*, vol. 16, no. 10, pp. 1217–1225, 1998.

[6] PA Bandettini, A Jesmanowicz, and EC Wong, "Processing strategies for time-course data sets in functional mri of the human brain," *Magnetic Resonance Medicine*, vol. 30, pp. 161–173, 1993.

[7] KJ Worsley, AC Evans, S Marrett, and P Neelin, "A three-dimensional statistical analysis for cbf activation studies in human brain," *Cerebral Blood Flow and Metabolism Journal*, vol. 12, pp. 900–918, 1992.

[8] GM Boynton, SA Engel, GH Glover, and DJ Heeger, "Linear systems analysis of functional magnetic resonance imaging in human v1," *Neuroscience Journal*, vol. 16, no. 13, pp. 4207–21, 1996.

[9] J Kershaw, BA Ardekani, and I Kanno, "Application of bayesian inference to fmri data analysis," *IEEE transactions on medical imaging*, vol. 18, no. 12, pp. 1138–1153, 1999.

[10] K-H Chuang, M-J Chiu, C-C Lin, and J-H Chen, "Model-free functional mri analysis using kohonen clustering neural network and fuzzy c-means," *IEEE transactions on medical imaging*, vol. 18, no. 12, pp. 1117–1128, 1999.

[11] S-C Ngan and X Hu, "Analysis of functional magnetic resonance imaging data using self-organizing mapping with spatial connectivity," *Magnetic Resonance in Medicine*, vol. 41, pp. 939–946, 1999.

[12] KJ Friston, P Jezzard, and R Turner, "The analysis of functional mri time-series," *Human Brain Mapping*, vol. 1, pp. 153–171, 1994.

[13] KJ Worsley, "An overview and some new developments in the statistical analysis of pet and fmri data," *Human Brain Mapping*, vol. 5, pp. 254–258, 1997.

[14] PP Mitra, S Ogawa, X Hu, and K Ugurbil, "The nature of spatiotemporal changes in cerebral hemodynamics as manifested in functional magnetic resonance imaging," *Magnetic Resonance in Medicine*, vol. 35, pp. 511–518, 1997.

[15] S-C Ngan, SM LaConte, and X Hu, "Temporal filtering of event-related fmri data using cross-validation," *Neuroimage*, vol. 2, pp, 797–804 2000.

[16] SM LaConte, S-C Ngan, and X Hu, "Wavelet transform based wiener filtering of event-related fmri data," *Magn. Reson. Med. (in press)*, 2000.

[17] AM Dale and RL Bruckner, "Selective averaging of rapidly presented individual trials using fmri," *Human Brain Mapping*, vol. 5, pp. 329–340, 1997.

[18] P Teo, G Sapiro, and B Wandell, "Creating connected representations of cortical gray matter for functional MRI visualization," *IEEE Trans. Medical Imaging*, vol. 16:06, pp. 852–863, December 1997.